Linkage Disequilibrium Estimation of Effective Population Size with Immigrants from Divergent Populations: A Case Study on Spanish Mackerel (*Scomberomorus commerson*)

Gilbert Michael Macbeth,*,[1] Damien Broderick,* Rik C. Buckworth,[†] and Jennifer R. Ovenden*
*Molecular Fisheries Laboratory, Queensland Government, St Lucia, Queensland, 4072, Australia, and [†]CSIRO Marine & Atmospheric Research, Wealth from Oceans National Research Flagship, Brisbane, Queensland, 4001, Australia

ABSTRACT Estimates of genetic effective population size (*Ne*) using molecular markers are a potentially useful tool for the management of endangered through to commercial species. However, pitfalls are predicted when the effective size is large because estimates require large numbers of samples from wild populations for statistical validity. Our simulations showed that linkage disequilibrium estimates of *Ne* up to 10,000 with finite confidence limits can be achieved with sample sizes of approximately 5000. This number was deduced from empirical allele frequencies of seven polymorphic microsatellite loci in a commercially harvested fisheries species, the narrow-barred Spanish mackerel (*Scomberomorus commerson*). As expected, the smallest SD of *Ne* estimates occurred when low-frequency alleles were excluded. Additional simulations indicated that the linkage disequilibrium method was sensitive to small numbers of genotypes from cryptic species or conspecific immigrants. A correspondence analysis algorithm was developed to detect and remove outlier genotypes that could possibly be inadvertently sampled from cryptic species or nonbreeding immigrants from genetically separate populations. Simulations demonstrated the value of this approach in Spanish mackerel data. When putative immigrants were removed from the empirical data, 95% of the *Ne* estimates from jacknife resampling were greater than 24,000.

The effective number in a breeding stock was defined by Wright (1930) as an idealized number of parents in a population that cause a given level of inbreeding or given change in allele frequencies. This effective number "is much smaller as a rule than the actual number of adult individuals" (Wright 1930) but is an important parameter in ecological studies because any change over time indicates underlying changes in population structure. The mean squared correlation of alleles at different loci is a measure of linkage disequilibrium, which can be used to estimate genetic effective population size ($\hat{N}e$) of diploid individuals. In small populations there is a greater correlation of alleles between loci compared with larger populations (Pudovkin *et al.* 1996; Hedgecock *et al.* 2007; Zhdanova and Pudovkin 2008) and hence there is a relationship with genetic effective population size (Waples 2006). It was suggested by Waples and Do (2010) that strong assortative mating would lead to biases in $\hat{N}e$. Later, Waples and England (2011) investigated migration between populations and concluded that the linkage disequilibrium method was robust to equilibrium migration with $\hat{N}e$, reflecting that of the local subpopulation. Waples and England (2011) also showed that pulse migration of strongly divergent individuals was found to depress estimates of local *Ne*.

The effect of pulse migration is an important finding because related factors could also lead to depressed *Ne* estimates. These factors could include inadvertent sampling of nontarget species and sampling of the same species but from populations that have become genetically divergent over many generations. Some fish species are known to exhibit natal philopatry, in which individuals have home spawning

Supporting information is available online at http://www.g3journal.org/lookup/suppl/doi:10.1534/g3.112.005124/-/DC1
[1]Corresponding author: Centre for Applications in Natural Resource Mathematics, School of Mathematics and Physics, The University of Queensland, Queensland, 4072 Australia. E-mail: gilbert.macbeth1@uq.net.au

		Female Gametes			
		A_jB_k	$A_jB_{k^*}$	$A_{j^*}B_k$	$A_{j^*}B_{k^*}$
Male Gametes	A_jB_k	2	1	1	1
	$A_jB_{k^*}$	1	0	1#	0
	$A_{j^*}B_k$	1	1#	0	0
	$A_{j^*}B_{k^*}$	1	0	0	0

The '#' indicates where A_jB_k combinations occur in genotypes but not gametes.

grounds but later disperse. Examples include herring, cod, sharks, swordfish, and anadromous salmonids (Beacham *et al.* 2005; Bekkevold *et al.* 2007; Svedang *et al.* 2007; Jorgensen *et al.* 2009; Smith and Alvarado-Bremer 2010). Under this model, samples from a single location taken when the species was in the dispersed phase could represent several genetically distinct (*i.e.*, mixed) stocks. The samples would not represent a panmictic population, causing deviations from the expected linkage disequilibria and a bias in the linkage disequilibrium estimation of *Ne*. For example, a downward bias in *Ne* estimates was simulated by Palstra and Ruzzante (2011) when divergent populations were pooled.

The frequency of natal philopatry is poorly known across marine species and virtually unknown in Australian fisheries species (Blower *et al.* 2012; Tillett *et al.* 2012). A species of considerable fisheries interest in Australia, and much of the Indo-West Pacific, is the narrow-barred Spanish mackerel, *Scomberomorus commerson*. It is a large, fast-swimming pelagic predator found throughout tropical and subtropical neritic waters of the Indo-West Pacific (Collette and Nauen 1983). If *S. commerson* exhibit natal philopatry, the mixing of genetically distinct populations within the sample collection area could depress *Ñe* in a similar manner suggested by pulse migration (Waples and England 2011). Seasonal aggregation for spawning followed by dispersal is supported by several lines of evidence: (1) seasonal variations in the availability of *S. commerson* (Buckworth *et al.* 2007), (2) a tag release study in northern Australia showing dispersal of recaptured fish with 12% more than 600 nautical miles away (Buckworth *et al.* 2007), (3) movement of fish on the eastern Australian coast southwards in summer presumably for feeding (McPherson 1988), and (4) multiple genetically distinct stocks in Southeast Asia (Fauvelot and Borsa 2011). The species is under active management throughout its range in Australia, and accurate estimates of effective population size have the potential to assist (Hare *et al.* 2011; Luikart *et al.* 2010; Ovenden *et al.* 2007; Palstra and Ruzzante 2008).

In this work we document a case study of the pitfalls associated with the estimation of *Ne* in *S. commerson* when large samples of genotypes ($S > 5000$) were sampled from a single location in northern Australia. We compare the estimated *Ne* from simulated populations with those from the empirical data. We critically review the estimates of *Ne* by testing hypotheses that the sampled population is a mixed stock. We also develop a method of screening and removing individuals likely to be from nontarget populations or species.

MATERIALS AND METHODS

Linkage disequilibrium estimation of effective population size (*Ñe*)

Linkage disequilibrium estimation of effective population size is derived from the correlation of alleles between loci. The correlation

is determined from allele frequencies and has the general form of the phi correlation coefficient

$$\hat{r}_{A_jB_k} = \frac{\hat{\Delta}_{A_jB_k}}{\sqrt{\left[\hat{p}_{A_j}\left(1 - \hat{p}_{A_j}\right) + \hat{D}_{A_j}\right]\left[\hat{p}_{B_k}\left(1 - \hat{p}_{B_k}\right) + \hat{D}_{B_k}\right]}}$$

(Weir 1996, p137) where $\hat{r}_{A_jB_k}$ is the estimated correlation between the jth allele in locus A and k^{th} allele in locus B given $\hat{p}_{A_j}$ is the empirical frequency estimation of allele j in locus A, $\hat{p}_{B_k}$ is the empirical frequency estimation of allele k in locus B, $\hat{D}_{A_j} = f(A_jA_j) - \hat{p}_{A_j}^2$ and $\hat{D}_{B_k} = f(B_kB_k) - \hat{p}_{B_k}^2$ represent the additional variance in allele frequencies due to deviations in Hardy Weinberg equilibrium, where $f()$ in the aforementioned formulae denote the observed homozygote frequencies. When diploid genotypes are sampled, the gametic phase is unknown with linkage disequilibrium determined by the Burrows estimate $\hat{\Delta}_{A_jB_k} = \hat{p}(A_jB_k) - 2\hat{p}_{A_j}\hat{p}_{B_k}$ (Schaid 2004). In this equation, $\hat{\Delta}_{A_jB_k}$ is the deviation from the estimated probability of A_jB_k gametes, $\hat{p}(A_jB_k)$, from their expected probability $2\hat{p}_{A_j}\hat{p}_{B_k}$. The value $\hat{p}(A_jB_k)$ had to be determined indirectly from the count of A_jB_k combinations within biallelic genotypes (Table 1) because the gamete frequencies A_jB_k were unknown. In Table 1, # indicates that there were no A_jB_k gametes present within the genotype; thus, the expected number of A_jB_k gametes given the genotype $A_jA_{j*}B_kB_{k*}$ is equal to $X_{A_j,A_{j*},B_k,B_{k*}}/2$, where $X_{A_j,A_{j*},B_k,B_{k*}}$ is the number of observed $A_jA_{j*}B_kB_{k*}$ genotypes. The estimated observed frequency of A_jB_k gametes summed from both intra- and intergametic loci is as follows:

$$p(A_jB_k) = \left[2X_{A_j,A_j,B_k,B_k} + X_{A_j,A_j,B_k,B_{k*}} + X_{A_j,A_{j*},B_k,B_k} + X_{A_j,A_{j*},B_k,B_{k*}}/2\right]/G$$

with X being the count of each genotype and G is the total number of gametes (Schaid 2004).

Under the assumption of unlinked and neutral loci, effective population size was estimated using linkage disequilibrium by correcting second-order terms for sampling error:

$$\hat{Ne} = \frac{1/3 + \sqrt{1/9 + 2.76\hat{r}^{2\prime}}}{2\hat{r}^{2\prime}} \tag{1}$$

where $\hat{r}^{2\prime} = \hat{r}^2 - E(\hat{r}^2_{sample})$, given $\hat{r}^2$ is the observed r-squared component calculated as the mean $\hat{r}^2_{A_jB_k}$ between all alleles over $L(L-1)/2$ pairwise comparisons of L loci, and $E(\hat{r}^2_{sample}) = [\frac{1}{S} + \frac{3.19}{S^2}]$ is the term correcting upward bias due to sampling S individuals (Waples 2006). The derivation of these equations was the subject of an entire article (Waples 2006); in summary $\hat{Ne}$ is a quadratic solution (equation 1) for *Ne* formed by equating $\hat{r}^{2\prime}$ to $\frac{1}{3Ne} - \frac{0.69}{Ne^2}$, where $\frac{1}{3Ne}$ is the drift term assuming loci are unlinked in a random mating population and $-\frac{0.69}{Ne^2}$ is a second-order correction determined by Waples (2006) using simulations.

Large undefined *Ne* estimates occur when the correction due to finite sample size $\hat{r}^2_{sample}$ is greater than $\hat{r}^2$, resulting in a negative *Ne* estimate. Negative estimates are plausible and indicate that the sample size S is too small, with the correction for sample size being larger than the $\hat{r}^2$ value determined from the data. *Ne* estimates were determined using program LDNE, where the lower 95% confidence intervals of $\hat{Ne}$ were determined by the jackknife method (Waples and Do 2008).

Built into the program of Waples and Do (2008) is a threshold called P_{crit}, which is used to exclude $\hat{r}^2_{A_jB_k}$ from the average $\hat{r}^2$ if $\hat{p}_{A_j}$ or $\hat{p}_{B_k}$ are below the P_{crit} threshold. Allele frequencies close to zero can bias $\hat{r}^2_{A_jB_k}$ (Waples 2006). We investigate $\hat{Ne}$ across a range of P_{crit} values because low-frequency alleles are more common in large

■ Table 2 Locus and allele frequency summary

Locus	S_L	Na	Maximum Allele Frequency	Number of Alleles With Frequencies		
				Greater Than 0.10	Between 0.01 and 0.001	Less Than 0.001
SCA30	5210	36	0.178	2	17	8
SM3	5206	32	0.183	4	8	13
SM37	4611	37	0.127	2	16	9
SCA47	4781	27	0.486	3	4	14
SCA49	4829	25	0.248	5	5	8
90RTE	5266	24	0.735	1	6	11
SCA8	5139	38	0.216	4	12	11

Sample size at each locus (S_L) and number of alleles (Na) for microsatellite loci used to genotype *S. commerson* with the maximum frequency and number of alleles within loci having frequencies less than or greater than the range shown.

datasets. Although the theory of Waples (2006) was tested using diallelic loci, it applies equally well in polymorophic data sets (Waples and Do 2010).

Collection of empirical data

Effective population size was estimated from genotypes of *S. commerson* individuals collected from a defined area, largely within 500 km northwest of Darwin, Northern Territory. Detailed genotyping methods are provided (Supporting Information, File S1).

Simulations with different effective population sizes

Ten-thousand replicate linkage disequilibrium *Ne* estimates were determined each for a range of population sizes *N* from 3000 to 60,000. The genotypes in each simulated population were generated using program SHAZA (http://molecularfisherieslaboratory.com.au/download-software/) (Macbeth *et al.* 2011). This program simulated *N* first-generation diploid genotypes by random sampling alleles within loci from the empirical allele frequencies of *S. commerson* from the Darwin population. The first *N*/2 genotypes were defined as females and the remainder males. Each individual in the next generation was simulated by random selection of a male and female with replacement. For each parental genotype and for all seven loci a single allele was randomly selected to create an individual diploid genotype. After this process, a total number of *N* individuals was created in four discrete generations.

In this design *N* is approximately equal to *Ne* (Waples 2006). In each replicate, *Ne* was estimated from 5413 generation four genotypes using a plan 2 sampling procedure (Waples 1989). Generation four was used to estimate *Ne* because this was sufficient for $\hat{r}^2$ to approach an asymptotic value (Sved 1971, Waples 2006). For example, the expectation of $\hat{r}^2$ in the first generation of simulated genotypes will be zero, resulting in upwardly biased estimates of *Ne*. Simulated genotypes have no missing loci; therefore, before estimating *Ne*, we introduced missing loci to emulate the empirical data structure that had missing loci. The missing loci were introduced for each and every

genotype in the simulated data by randomly drawing with replacement a genotype in the empirical data and deleting all loci in the simulated genotype that were found to be missing in the empirical genotype sampled.

Ne estimates from empirical data with outlier genotypes removed

Putative "outlier" genotypes, defined as genotypes not originating from the focal population under investigation, were identified and removed from the empirical data using a correspondence analysis (CA). The CA algorithm used here was developed in a pilot study by visual assessment of simulated outliers from plots of the first two principal components of a singular value decomposition. Up to 10 CA iterations were performed with iterations continuing until no further outliers are found. In each iteration, outlier genotypes were defined when principal components *PC1* and *PC2* (Appendix A) satisfied a threshold $\sqrt{(PC1 + PC2)} > 2$, which removed outliers furthest from the central cluster.

Ne estimates from empirical data with outlier genotypes removed and genotypes from nontarget species added

To test the sensitivity of *Ne* estimates in genotype samples containing nontarget species, a test was conducted by adding 100 genotypes of a nontarget species (gray mackerel, *Scomberomorus semifasciatus*) to the "cleaned" *S. commerson* data. We would anticipate that adding foreign genotypes will increase $\hat{N}e$ bias and indirectly show that cleaning the data could reduce bias in empirical data estimates. *Scomberomorus semifasciatus* genotypes amplified at five of the seven *S. commerson* loci with alleles at loci SCA47 and SCA49 marked as missing.

Simulation of genetically divergent populations

To further test the efficiency of the CA algorithm for detecting outlier genotypes, we considered 10 simulated populations that diverged from a founding population across numerous generations. The allele

■ Table 3 Estimates of LDNE effective population size ($\hat{N}e$) in *S. commerson*

	P_{crit}						
	0.05	0.02	0.01	0.001	0.0005	0.0001	0.0000
$\hat{N}e$	−40,163[a]	−799,447	79,842	17,503	3584	503	418
$\hat{N}e_{lower}$	19,595	24,728	22,209	12,759	3290	489	406
$\hat{N}e_{upper}$	Infinite	Infinite	Infinite	27,158	3921	517	428

$\hat{N}e$ at different P_{crit} thresholds with the upper and lower 95% confidence intervals.
[a] Negative $\hat{N}e$ estimates indicate a large undefined *Ne*.

frequencies of the founding population matched those from empirical *S. commerson* samples. Population size was set at $N = 10,000$ and after 100, 200, 500, 1000, or 2000 generations, the population was sampled (sample size of 5413 genotypes). As described previously, the program SHAZA was used to generate N genotypes of the founding population. This was followed by creating N genotypes each successive generation from random sampling of parental alleles as described previously using an equal sex ratio. Pairwise F_{ST} values were determined between divergent, simulated populations using Genetix 4.05 software (Belkhir *et al.* 1996−2004). For each of the 10 populations, 100 samples were randomly removed and replaced by 100 random genotypes selected from one of the other nine populations. Following this procedure, we had $n = 90$ populations with 100 immigrant genotypes from nontarget populations and $n = 10$ populations with no immigrants. Ne was estimated before and after the data were cleaned using CA.

The ability of the CA algorithm to identify immigrants was compared with the Bayesian clustering approach of STRUCTURE, version 2.3.3 (Pritchard *et al.* 2000). STRUCTURE analysis was applied to the 90 populations that contained 100 immigrants after diverging 2000 generations. Runs were performed by specifying: $k = 2$ clusters, an admixture ancestry model with allele frequencies correlated and a burn in length of 100,000 iterations followed by 100,000 MCMC iterations. One sample location was assumed with no location prior possible.

RESULTS

Empirical data

The majority of the 5413 *S. commerson* samples were genotyped with all seven loci (71%), but some samples were genotyped with either six (12%), five (10%), and four (7%) polymorphic microsatellite loci. The numbers of alleles per microsatellite locus varied from 24 (90RTE) to 38 (SCA8), with 65% of alleles across all loci having frequencies less than or equal to 0.01 (Table 2). These low-frequency alleles were selectively removed from data used to estimate Ne by the LDNe software depending on the chosen P_{crit} thresholds (for more details see: Supplementary genotype results).

Against expectations, LDNE estimates ($\hat{N}e$) from empirical data varied systematically across P_{crit} values (Table 3). As the P_{crit} threshold decreased in magnitude, so too did the magnitude of non-negative estimates of Ne. This covariance raised doubts about setting P_{crit} to $1/(2S) = 1/(2 \times 5413) \sim 0.0001$, where all singleton alleles would be removed, and the general effectiveness of removing low-frequency alleles for the estimation of Ne. The lower confidence interval of $\hat{N}e$ was more stable than the mean estimates but still varied widely from 406 to 24,728 and as such provided no informative value of the lower bound of $\hat{N}e$.

Simulations with different effective population sizes

Simulations indicated that 5413 genotype samples should be sufficient to estimate effective population size if the true size was 3000 and 10,000 (Figure 1 and Figure 2). Simulations with $N = 3000$ (Figure 1) had no extreme estimates of Ne, whereas simulations with $N = 10,000$ (Figure 2) had a small number of outlier estimates that were greater than 40,000 or less than minus 20,000. In Figures 1 and 2, P_{crit} values between 0.01 and 0.001 gave the smallest SD of $\hat{N}e$, illustrating the importance of removing the majority of low frequency alleles.

As expected, simulations with $N = 100$ and $N = 1000$ (Figure S1 and Figure S2) gave more precise estimates of Ne than with $N = 3000$ (Figure 1). Increasing N from 10,000 to 30,000 and 60,000 (Figure 2;
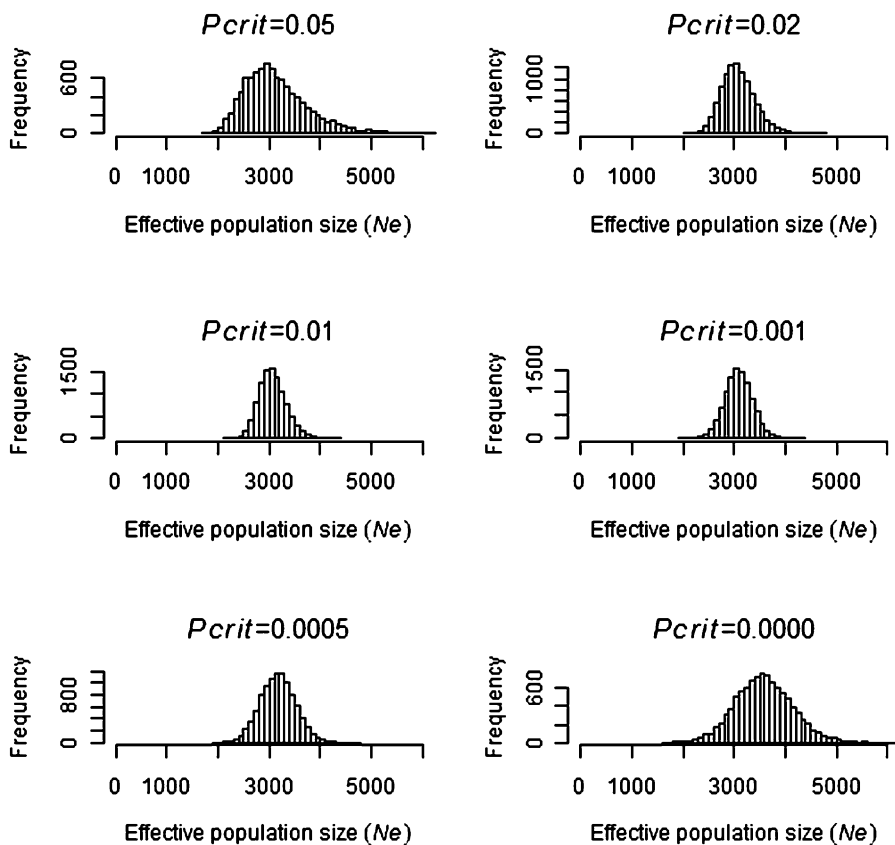

Figure 1 Frequency of 10,000 Ne estimates when simulating a population size of $N = 3000$ at different P_{crit} values.
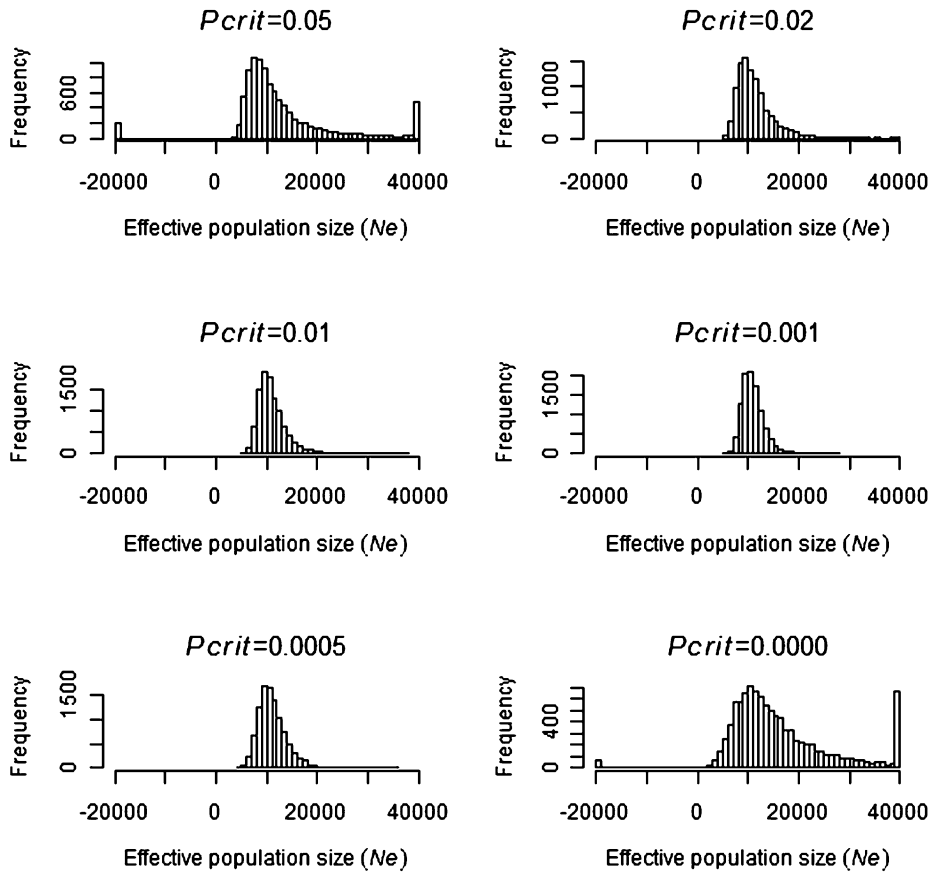
Figure 2 Frequency of 10,000 Ne estimates when simulating a population size of $N = 10,000$ at different P_{crit} values. The frequency of all Ne estimates less than 20,000 and greater than 40,000 were pooled and are indicated on the x-axis limits of each graph.

Figure S3, and Figure S4) resulted in a lower precision of $\hat{N}e$ with a greater number of negative and extremely large estimates of Ne. An interesting finding was that, at large N values such as 60,000, the lower 95% confidence interval (Figure S5) was more precise than the expected mean value (Figure S4), particularly at P_{crit} values around 0.01. The results indicate that we had sufficiency in the data to detect the lower 95% confidence interval if N was equal to 60000 with the mean lower confidence interval being 22,188 (P_{crit} = 0.01).

It is important to note that the smallest 1% of $\hat{N}e$ using P_{crit} = 0.0000 determined from the 100th-ranked positive value was 4134, 5308, and 5846 when N was 10,000, 30,000, and 60,000, respectively, which revealed an anomaly between the simulation results and empirical data estimates of $\hat{N}e$. If the true Ne was larger than 10,000, then the smallest $\hat{N}e$ estimate expected at P_{crit} = 0.0000 would be greater than 4134 ($P < 0.01$), which differs from the empirical estimate of 418. Conversely, if the true Ne was smaller than or equal to 10,000, then simulations indicated that no negative estimates of $\hat{N}e$ would be expected at P_{crit} = 0.02 ($P < 0.0001$), which was contrary to that observed from empirical data with $\hat{N}e$ = -799447 (Table 3). This finding highlighted that there was a significant difference between the empirical and simulated data, which was subsequently investigated by examining outlier genotypes.

Ne estimates from empirical data with outlier genotypes removed

The removal of putative outlier genotypes from empirical *S. commerson* data took nine *CA* iterations before there were no genotypes exceeding the $\sqrt{(PC1 + PC2)} > 2$ threshold (Figure S6). An order of magnitude increase in $\hat{N}e$ (Table 4) was observed after the first

iteration, which removed just 33 outliers (0.6% of total number of genotypes). This finding indicated that putative outlier genotypes can significantly bias Ne estimates in empirical data.

After the nine *CA* iterations, 3.2% of samples were removed. Subsequent Ne estimates on the cleaned data were negative at all P_{crit} thresholds, except when P_{crit} was 0.01 ($\hat{N}e$ = 550582). This finding indicated that a P_{crit} of 0.01 provided the greatest accuracy, as it had the smallest confidence interval assessed by the fact that it was the only P_{crit} value in which the correlation of alleles between loci was greater than that expected from sampling error. At this P_{crit} value $\hat{N}e$ was relatively stable at around 80,000 to 100,000 until the last two iterations with $\hat{N}e$ increasing to 550,582. When P_{crit} was 0.01, the harmonic mean of $\hat{N}e$ across all nine iterations was 110,000.

The lower 95% confidence interval of the Ne estimates ($\hat{N}e_{lower}$) from Table 4 is reported in Table 5. The lower confidence intervals appeared to be more stable than the estimates provided in Table 4 when the P_{crit} values were equal to or greater than 0.001. The range of $\hat{N}e_{lower}$ estimates when P_{crit} = 0.01 were within 21% of each other with a harmonic mean of 24000.

Ne estimates from empirical data with outlier genotypes removed and genotypes from nontarget species added

Adding nontarget species (gray mackerel, *S. semifasciatus*) to the "cleaned" *S. commerson* data significantly reduced Ne estimates (Table 6). Considering the total sample size was 5413, the results clearly show that only a small proportion of nontarget species can have a large impact on linkage disequilibrium estimates of Ne. For example, adding as few as eight (0.15%) *S. semifasciatus* genotypes resulted in a 5.7-fold

CA Iteration (Removed)	P_{crit}						
	0.05	0.02	0.01	0.001	0.0005	0.0001	0.0000
0 (0)	−40,163[a]	−799,447	79,842	17,503	3584	503	418
1 (33)	−32,062	−117,650	90,318	112,421	55,074	4968	5051
2 (38)	−33,926	−114,426	91,549	104,569	53,546	8082	7947
3 (51)	−34,571	−104,127	93,996	105,937	48,611	8838	9495
4 (60)	−37,447	−99,305	86,818	113,630	51,105	133,636	171,370
5 (90)	−38,487	−86,051	89,982	302,878	−448,815	−51,226	−36,471
6 (119)	−35,678	−76,242	120,453	302,946	−146,528	−38,189	−30,685
7 (153)	−38,909	−75,672	101,714	610,512	−69,972	−16,082	−16,082
8 (170)	−32,038	−65,015	296,541	−795,394	−58,191	−14,132	−14,132
9 (174)	−32,371	−67,105	550,582	−420,513	−48,637	−14,059	−14,059

The removal of putative outliers from nine sequential CA iterations with the cumulative number of genotypes removed indicated in brackets and the following estimates of *Ne* at different P_{crit} thresholds. CA, correspondence analysis.
[a] Negative *Ne* estimates indicate a large undefined *Ne*.

reduction in $\hat{N}e$ when $P_{crit} = 0.01$. All of the 200 nontarget gray mackerel genotypes were identified and removed by the first iteration of CA analysis compared with the nine iterations that were required with the empirical data (Table 4). This finding suggests that the putative outliers in the empirical data were more similar to *S. commerson* than *S. semifasciatus*.

Our *S. semifasciatus* samples did not amplify at loci SCA47 and SCA49. Removing all genotypes in the empirical data that did not amplify at these two loci produced a similar $\hat{N}e$ profile to Table 3, indicating that *S. semifasciatus* cannot be solely implicated in the anomaly between the simulated and empirical data.

Simulation of genetically divergent populations
Ten populations simulated after divergence from a common founder population had average pairwise F_{ST} values of 0.004, 0.010, 0.027, 0.048, and 0.091 after 100, 200, 500, 1000, and 2000 generations, respectively. With no mixing of the populations during genotype sampling, *Ne* estimates approximated the simulated population size ($N = 10,000$, Table 7).

Ninety populations with 100 immigrants were created from pairs of the 10 divergent populations. Across these 90 populations CA analysis found an average (SD) of 7 (4), 18 (8), 44 (12), 74 (12), and 93 (6) immigrants after 100, 200, 500, 1000, and 2000 generations, respectively. The average number of CA iterations required before no more immigrants could be detected were 3.4, 3.6, 3.6, 3.1, 3.0 after 100, 200, 500, 1000, and 2000 generations, respectively. As a compar-

ison, the program STRUCTURE was not able to distinguish the immigrants, even after 2000 generations of divergence. When two populations were specified in STRUCTURE 97 of the 100 immigrants and 47.3% of the remaining 5313 samples were partitioned into the same population. This finding indicated that there was not sufficient genetic divergence between the populations to cluster the small proportion of immigrants into a separate population.

In the presence of 100 immigrants, there was a downward bias in $\hat{N}e$ of the focal population for P_{crit} values of 0.00 and 0.01 (Table 7) as the number of generations of divergence increased. After outlier genotypes were removed *Ne* estimates were more consistent with an expected value of $N = 10,000$. After outlier (*i.e.*, immigrant) genotypes were removed by CA, the smallest bias and highest accuracy of *Ne* occurred when $P_{crit} = 0.01$.

DISCUSSION
Palstra and Ruzzante (2011) urged further theoretical developments to avoid a downward bias in estimating linkage disequilibrium *Ne* in naturally occurring metapopulations. Our results have demonstrated that under certain circumstances even estimates for focal populations can be downwardly biased. We believe this bias could be due to the presence of 1) nontarget species and 2) immigrant genotypes from diverged populations among the samples taken for estimation. Importantly, only a few 'contaminant' genotypes can severely bias *Ne* estimates.

The nature of how the contaminant genotypes differ is at the crux of what causes the downward bias in effective population size. We

■ Table 5 Lower 95% confidence interval of *Ne* from *S. commerson* genotypes

CA Iteration (Removed)	P_{crit}						
	0.05	0.02	0.01	0.001	0.0005	0.0001	0.0000
0 (0)	19,595	24,728	22,209	12,759	3290	489	406
1 (33)	22,540	30,509	22,943	26,461	17,594	1988	2046
2 (38)	21,571	30,713	23,011	26,119	17,498	2849	2913
3 (51)	21,232	31,541	23,144	33,737	25,337	7606	8131
4 (60)	20,110	31,970	22,720	26,879	16,904	16,696	14,799
5 (90)	19,615	33,487	22,809	42,238	60,094	−271,390[a]	−83,353
6 (119)	20,379	35,118	24,305	29,804	53,307	−98,902	−59,311
7 (153)	19,174	34,947	23,471	31,098	80,748	−35,452	−35,453
8 (170)	21,646	37,832	27,703	36,446	151,392	−23,066	−23,066
9 (174)	21,445	37,064	28,922	35,858	−615,338	−23,260	−23,260

The removal of putative outliers from nine CA iterations with the cumulative number of genotypes removed indicated in brackets and the following estimates of the lower 95% confidence interval ($\hat{N}e_{lower}$) at different P_{crit} thresholds. CA, correspondence analysis.
[a] Negative *Ne* estimates indicate a large undefined *Ne*.

■ **Table 6 Effect of *S. commerson* Ne estimates when adding nontarget species**

Gray Mackerel Genotypes Added	P_{crit}						
	0.05	0.02	0.01	0.001	0.0005	0.0001	0.0000
0	−32,371[a]	−67,105	550,582	−420,513	−48,637	−14,059	−14,059
1	−32,382	−67,686	566,612	−410,564	−48,310	1303	1303
2	−32,315	−67,583	719,220	−356,551	−47,594	1031	1031
4	−35,620	−70,777	159,027	−966,684	−50,839	1138	1138
8	−36,871	−79,371	95,957	206,370	3930	1179	1179
16	−37,624	−94,247	43,218	2030	1088	1238	1238
32	−45,964	−1,040,355	16,140	1104	985	1233	1233
64	626,218	5420	2896	700	776	974	1014
100	23,439	5946	813	553	654	806	862
200	2189	418	233	376	455	547	620

Starting with *S. commerson* data with 174 outliers removed by nine CA iterations, Ne estimates at different P_{crit} thresholds were determined after progressive addition of gray mackerel (*S. semifasciatus*) genotypes. CA, correspondence analysis.

[a] Negative Ne estimates indicate a large undefined Ne.

assumed that contaminant genotypes were from transient individuals that did not interbreed among members of the focal population. Our results are therefore not in disagreement with a study in which the authors showed that linkage disequilibrium estimates of effective population size are robust to populations displaying equilibrium migration and mating over many generations (Waples and England 2011). We propose the bias expectations are different for contamination by unrelated species or reproductively isolated subpopulations *vs.* subpopulations from the same metapopulation.

The CA algorithm performed well in identifying and removing nontarget genotypes that were added to simulated population samples. In our hands, standard methods of population clustering such as STRUCTURE (Pritchard *et al.* 2000) were incapable of identifying the simulated immigrants. The threshold value of 2 used in the CA algorithm was developed by trial and error as a reasonable threshold to exclude outlier genotypes without removing too many target population genotypes. A series of scatter plots on principal coordinates is shown after each iteration of removing outliers on the threshold (Figure S6). The pattern in this series was typical for many of the simulations runs in which a final cluster of points becomes clearly visible. As expected, as the F_{ST} between nontarget and the target populations decreased, it was more difficult to detect the nontarget genotypes using the CA algorithm. Although the simulated results seem sensible,

the theoretical basis of this algorithm and its generalizability to removing nontarget genotypes in other data sets would provide additional support for this method. Our findings suggest that it is worthwhile to detect and remove putative nontarget genotypes prior to LDNE analysis.

Our simulated divergent populations were implemented using a simple Wright-Fisher model with mating modified such that gametes were chosen from populations having equal numbers in each sex. This model was used by Waples (2006); however, many other models could have been used, including those with mutation and selection (Der *et al.* 2011). These additional processes would cause a larger divergence at the same number of generations compared with the simple genetic drift model used in our study.

Our investigation suggests that mackerel genotypes collected around Darwin contained a small proportion from genetically divergent *S. commerson* population(s) or from congeneric species. It is possible that tissue samples of closely related species were taken inadvertently, thus mimicking an admixed *S. commerson* population. Our 100 gray mackerel (*S. semifasciatus*) samples amplified at five of the seven loci used in our study, whereas another closely related endemic species (*Scomberomorus queenslandicus*) amplifies at all the seven loci (unpublished data). The fact that all gray mackerel genotypes were successfully removed by our CA method does indicate that

■ **Table 7 Harmonic mean of Ñe before and after outlier genotypes removed**

	Before Outlier Genotypes Removed		After Outlier Genotypes Removed	
Generations	No Immigrants, *n* = 10	With Immigrants, *n* = 90	No Immigrants, *n* = 10	With Immigrants, *n* = 90
P_{crit} = 0.000				
100	9896	6236	13,911	17,100
200	10,543	3037	11,947	13,973
500	10,029	1282	11,151	11,558
1000	97,734	571	10,548	11,049
2000	11,834	176	12,359	12,295
P_{crit} = 0.010				
100	10,732	11,096	10,841	11,267
200	10,557	10,932	10,670	11,094
500	10,211	9420	10,217	10,003
1000	9595	7629	9691	9736
2000	10,407	4456	10,508	10,564

Harmonic mean of Ñe at two P_{crit} thresholds in simulated populations with N = 10,000 and sample size S = 5413 containing no immigrants or with 100 genotypes drawn from a single immigrant population. The immigrants are from populations diverging after a different number of generations from a common population. The harmonic mean in each column was based on *n* separate Ñe estimates before and after outlier genotypes were removed using the CA algorithm. CA, correspondence analysis.

our methods work well when nontarget species are implicated. We would expect intermediate results when populations are at varying levels of population divergence as indicated by our simulations.

We assumed no genotyping errors when estimating linkage disequilibrium, although prescreening of the data resulted in one locus being removed due to a deviation from Hardy Weinberg equilibrium. Although this deviation might indicate the presence of a null allele error, there could be other errors, such as allelic dropout errors. Random dropout errors are not expected to change the expectation of linkage disequilibrium estimates nor the outcome of the expected Ne estimate.

Assuming that all samples represented *S. commerson*, it is likely that the population adjacent to Darwin is an admixed population containing small numbers of individuals from genetically distinct populations. These individuals could also have been transient vagrants of genetically distinct populations of *S. commerson* (Sulaiman and Ovenden 2010; Fauvelot and Borsa 2011) that were sampled in the same geographical region. The hypothesis that a small (rather than large) number of immigrant genotypes were present in the empirical genotypes is supported by the observations that (1) most adults in a mark-recapture study were found to move less than 100km per year parallel to the shore and (2) isotope signatures in the sagittal otolith carbonate of *S. commerson* indicated spatial separation across northern Australia (Newman *et al.* 2009).

In our *S. commerson* data, it was very difficult to get a precise estimate of $\hat{N}e$. Before "cleaning" the data with CA, Ne estimates varied at different P_{crit} levels, including some negative estimates of Ne. Using a P_{crit} value of 0.01 the likely $\hat{N}e$ seems very large with an estimate of 110,000 from empirical data. We believe this estimate to be unreliable as inferred from the lack of sufficiency of the data when estimating the mean Ne with $N = 600,000$ (Figure S4).

Negative estimates of Ne are counterintuitive and indicate that the true Ne is large and undefined. Waples and Do (2010) point out that even if the Ne estimate is negative, if adequate data are available, the lower bound of the confidence interval may be finite and can provide useful information. This finding was also supported by our simulations with large N values in which the lower 95% confidence interval for *S. commerson* appears to be much more stable than the estimate and upper limits. Using a P_{crit} value of 0.01, we found that the lower 95% confidence interval gave a harmonic mean of $\hat{N}e = 24000$ from empirical data. More loci could be used to achieve more precise estimates of Ne. However, we had sufficiency in the data to detect Ne when $N = 30,000$ (Figure S3, $P_{crit} = 0.01$). We also had sufficiency in the data when estimating the lower 95% confidence of Ne with $N = 60,000$ giving $\hat{N}e_{lower} = 22188$ (Figure S5, $P_{crit} = 0.01$). We conclude from these simulations that the empirical Ne_{lower} estimate of 24,000 is reasonably reliable. In ecological terms 24,000 represents a large and stable genetic population size, and we would expect to reach a similar conclusion with the addition of more loci.

This study was primarily focused on the bias in the linkage disequilibrium estimation of Ne when a population may include genetically divergent conspecifics. There are many other approaches used to estimate Ne that have different underlying assumptions (Barker 2011) and that should be evaluated as being suitable for the estimation of Ne in large, naturally occurring populations. A natural progression in this area of research is to develop inferences of census population sizes based on effective size estimates (Palstra and Ruzzante 2008) and how these could be used to assist management of natural resource species.

Realistic simulations have showed that it is possible to make effective population size estimates using the linkage disequilibrium method with finite confidence limits up to several thousand depending on the number of loci and genotypes assayed. Estimates of effective size made from samples taken from naturally occurring populations must be treated with caution. We recommend pretreatment of the sampled genotypes to identify outliers, particularly if the population being studied is sympatric with closely related species, or is possibly receiving immigrants from adjacent populations.

LITERATURE CITED

Barker, J. S. F., 2011 Effective population size of natural populations of *Drosophila buzzatii*, with a comparative evaluation of nine methods of estimation. Mol. Ecol. 20: 4452–4471.

Beacham, T. D., J. R. Candy, B. McIntosh, C. MacConnachie, A. Tabat *et al.*, 2005 Estimation of stock composition and individual identification of Sockeye salmon on a Pacific rim basis using microsatellite and major histocompatibility complex variation. Trans. Am. Fish. Soc. 134: 1124–1146.

Bekkevold, D., L. A. W. Clausen, S. Mariani, C. Andre, T. B. Christensen *et al.*, 2007 Divergent origins of sympatric herring population components determined using genetic mixture analysis. Mar. Ecol. Prog. Ser. 337: 187–196.

Belkhir, K., P. Borsa, L. Chikhi, N. Raufaste, and F. Bonhomme, 1996–2004 GENETIX 4.05, logiciel sous Windows TM pour la genetique des populations. Laboratorie Genome, Populations, Interactions, CNRS UMR 5171, Universite de Montpellier II, Montpellier (France). Available at: http://kimura.univ-montp2.fr/genetix/. Accessed: March 5, 2013.

Blower, D. C., J. M. Pandolfi, M. C. Gomez-Cabrera, B. D. Bruce, and J. R. Ovenden, 2012 Population genetics of Australian white sharks reveals fine-scale spatial structure, transoceanic dispersal events and low effective population sizes. Mar. Ecol. Prog. Ser. 455: 229–244.

Buckworth, R. C., S. J. Newman, J. R. Ovenden, R. J. G. Lester, and G. R. McPherson, 2007 The stock structure of northern and western Australian Spanish mackerel. Department of Primary Industry, Fisheries and Mines, Darwin, Australia. Fishery Report No. 88.

Buckworth, R. C., J. R. Ovenden, D. Broderick, G. M. Macbeth, G. R. McPherson *et al.*, 2012 GENETAG: Genetic mark-recapture for real-time harvest rate monitoring: Pilot studies in Northern Australia Spanish Mackerel fisheries. Northern Territory Government, Queensland, Australia. Fishery Report No. 107.

Collette, B. B., and C. E. Nauen, 1983 *FAO Species Catalogue. Vol. 2. Scombrids of the World. An Annotated and Illustrated Catalogue of Tunas, Mackerels, Bonitos and Related Species Known to Date.* Food and Agriculture Organization Fish Synopsis No. 125, Rome.

Der, R., C. L. Epstein, and J. B. Plotkin, 2011 Generalised population models and the nature of genetic drift. Theor. Popul. Biol. 80: 80–99.

Fauvelot, C., and P. Borsa, 2011 Patterns of genetic isolation in a widely distributed pelagic fish, the narrow-barred Spanish mackerel (*Scomberomous commerson*). Biol. J. Linn. Soc. Lond. 104: 886–902.

Hare, M. P., L. Nunney, M. K. Schwartz, D. E. Ruzzante, M. Burford *et al.*, 2011 Understanding and estimating effective population size for practical application in marine species management. Conserv. Biol. 25: 438–449.

Hedgecock, D., S. Launey, A. I. Pudovkin, Y. Naciri, S. Lapegue *et al.*, 2007 Small effective number of parents (N-b) inferred for a naturally spawned cohort of juvenile European flat oysters *Ostrea edulis*. Mar. Biol. 150: 1173–1182.

Jorgensen, S. J., C. A. Reeb, T. K. Chapple, S. Anderson, C. Perle *et al.*, 2010 Philopatry and migration of Pacific white sharks. Proc. Biol. Sci. B. 277: 679–688.

Luikart, G., N. Ryman, D. A. Tallmon, M. K. Schwartz, and F. W. Allendorf, 2010   Estimation of census and effective population sizes: the increasing usefulness of DNA-based approaches. Conserv. Genet. 11: 355–373.

Macbeth, G. M., D. Broderick, J. R. Ovenden, and R. C. Buckworth, 2011   Likelihood-based genetic mark-recapture estimates when genotype samples are incomplete and contain typing errors. Theor. Popul. Biol. 80: 185–196.

McPherson, G. R., 1988   A review of large coastal pelagic fishes in the South Pacific Region, with special reference to *Scomberomorus commerson* in North-East Australian waters [WP 15]. Noumea: SPC. Workshop on Pacific Inshore Fishery Resources, Noumea, New Caledonia, March 14-25, 1988.

Nenadic, O., and M. Greenacre, 2006   Computation of multiple correspondence analysis, with code in R, pp. 523–551 in *Multiple Correspondence Analysis and Related Methods*, edited by M. J. Greenacre, and J. Blasius. Chapman & Hall/CRC Press, Boca Raton, FL.

Newman, S. J., R. C. Buckworth, M. Mackie, P. Lewis, I. Wright *et al.*, 2009   Spatial subdivision of adult assemblages of Spanish mackerel, *Scomberomorus commerson* (Pisces: Scombridae) across northern Australia: implications for fisheries management. Glob. Ecol. Biogeogr. 18: 711–723.

Ovenden, J., D. Peel, R. Street, A. J. Courtney, S. D. Hoyle *et al.*, 2007   The genetic effective and adult census size of an Australian population of tiger prawns (*Penaeus esculentus*). Mol. Ecol. 16: 127–138.

Palstra, F. P., and D. E. Ruzzante, 2008   Genetic estimates of contemporary effective population size: what can they tell us about the importance of genetic stochasticity for wild population persistence? Mol. Ecol. 17: 3428–3447.

Palstra, F. P., and D. E. Ruzzante, 2011   Demographic and genetic factors shaping contemporary metapopulation effective size and its empirical estimation in salmonid fish. Heredity 107: 444–455.

Pritchard, J. K., M. Stephens, and P. Donnelly, 2000   Inference of population structure using multilocus genotype data. Genetics 155: 945–959.

Pudovkin, A. I., D. V. Zaykin, and D. Hedgecock, 1996   On the potential for estimating the effective number of breeders from heterozygote excess in progeny. Genetics 144: 383–387.

R Development Core Team, 2011   R: A language and environment for statistical computing. R Foundation for Statistical Computing, Vienna, Austria.

Schaid, D. J., 2004   Linkage disequilibrium testing when linkage phase is unknown. Genetics 166: 505–512.

Smith, B. L., and J. R. Alvarado-Bremer, 2010   Inferring population admixture with multiple nuclear genetic markers and Bayesian genetic clustering in Atlantic swordfish (*Xiphlas gladius*). Coll. Vol. Sci. Pap. ICCAT 65: 185–190.

Sulaiman, Z. H., and J. R. Ovenden, 2010   Population genetic evidence for the east–west division of the narrow-barred Spanish mackerel (*Scomberomorus commerson*, Perciformes: Teleostei) along Wallace's Line. Biodivers. Conserv. 19: 563–574.

Sved, J. A., 1971   Linkage disequilibrium and homozygosity of chromosome segments in finite populations. Theor. Popul. Biol. 2: 125–141.

Svedang, H., D. Righton, and P. Jonsson, 2007   Migratory behaviour of Atlantic cod *Gadus morhua*: natal homing is the prime stock-separating mechanism. Mar. Ecol. Prog. Ser. 345: 1–12.

Tillett, B. J., M. G. Meekan, I. C. Field, D. C. Thorburn, and J. R. Ovenden, 2012   Evidence for reproductive philopatry in the bull shark, *Carcharhinus leucas* in northern Australia. J. Fish Biol. 80: 2140–2158.

Waples, R. S., 1989   A generalized approach for estimating effective population size from temporal changes in allele frequency. Genetics 121: 379–391.

Waples, R. S., 2006   A bias correction for estimates of effective population size based on linkage disequilibrium at unlinked gene loci. Conserv. Genet. 8: 167–184.

Waples, R. S., and C. Do, 2008   LDNE: a program for estimating effective population size from data on linkage disequilibrium. Mol. Ecol. Resources. 8: 753–756.

Waples, R. S., and C. Do, 2010   Linkage disequilibrium estimates of contemporary Ne using highly variable genetic markers: a largely untapped resource for applied conservation and evolution. Evol. Applications 3: 244–262.

Waples, R. S., and P. R. England, 2011   Estimating contemporary effective population size on the basis of linkage disequilibrium in the face of migration. Genetics 189: 633–644.

Weir, B., 1996, p. 137 in *Genetic Data Analysis II*. Sinauer Associates, Sunderland, MA.

Wright, S., 1930   Evolution in mendelian populations. Genetics 16: 97–159.

Zhdanova, O., and A. I. Pudovkin, 2008   Nb_HetEx: a program to estimate the effective number of breeders. J. Hered. 99: 694–695.

Communicating editor: P. Pfaffelhuber

APPENDIX A

CA R script

The genotype file is presented as an incidence matrix Z having columns for each allele within every locus. For each and every genotype a single row marking the presence '1' or absence '0' of each allele present within each column is appended to fill the content of the Z matrix. The R code modified from Nenadic and Greenacre (2006) converts the incidence matrix to a format that can be read and manipulated by R (R Development Core Team 2011) with the first two principal components *PC1* and *PC2* determined as follows:

```
Z <- data.matrix(Z)     # convert to matrix
P <- Z / sum(Z)     # proportional contribution
rm <- apply(P, 1, sum)     # sum rows
cm <- apply(P, 2, sum)     # sum columns
eP <- rm %*% t(cm)     # multiply by transpose
dec <- svd((P - eP) / sqrt(eP))     # singular value decomposition
PC1 <- dec$u[,1] * dec$d[1] / sqrt(rm)     # Principal component 1
PC2 <- dec$u[,2] * dec$d[2] / sqrt(rm)     # Principal component 2
```